Publ. Astron. Soc. Japan 39, 685–708 (1987)

A Nuclear Molecular Ring and Gas Outflow in the Galaxy M82

Naomasa NAKAI, Masahiko HAYASHI,* Toshihiro HANDA,
Yoshiaki SOFUE,* and Tetsuo HASEGAWA

Nobeyama Radio Observatory,†
Minamimaki-mura, Minamisaku-gun, Nagano 384-13

and

Minoru SASAKI

Department of Astronomy, Faculty of Science,
University of Kyoto, Sakyo-ku, Kyoto 606

(Received 1986 September 19; accepted 1987 June 7)

Abstract

The CO ($J=1$–0) emission of M82 has been mapped with spatial resolution of 16″. The main-beam brightness temperature near the center is as high as 5.8 K. The mass of the molecular gas in the mapped area of 1′.5 (1400 pc) square is estimated to be $1.1\times10^{8}M_{\odot}$, which shares 10% of the dynamical mass. The CO intensity in the central region of M82 has two peaks, which we interpret in terms of a ring of the molecular gas with a radius of 200 pc. This "200-pc ring" extends from $r=80$ pc to 400 pc. The molecular ring corresponds to the sites of current star formation. Spurlike structures of the molecular gas emerge perpendicularly to the galactic plane toward the halo and extend more than 500 pc from the disk. The spurs are located just outside the ridges of Hα filaments and X-ray halos, and may indicate a hollow cylinder perpendicular to the disk. This cylinder has a vertical velocity gradient. We propose a model in which the molecular gas in M82 as well as the hot plasma is expelled from the plane of the galaxy at a velocity of 100–500 km s^{-1}, most likely 200 km s^{-1}. The implied mechanical energy [$(1$–$13)\times10^{55}$ erg] of the expelled gas can be explained by the energy supplied by successive supernova explosions in the central region of the galaxy.

Key words: Galaxies; Interstellar molecules; M82; Star formation.

* Present address: Department of Astronomy, Faculty of Science, University of Tokyo, Bunkyo-ku, Tokyo 113.

† Nobeyama Radio Observatory, a branch of the Tokyo Astronomical Observatory, University of Tokyo, is a facility open for general use by researchers in the field of astronomy, astrophysics, and astrochemistry.

1. Introduction

M82 (NGC 3034, 3C 231) is a well-known peculiar galaxy, classified as Irr II (Holmberg 1950, 1958; Sandage 1961) or I0 (de Vaucouleurs and de Vaucouleurs 1964). Luminous H II regions, star clusters, and patchy dark lanes are mixed on the plane of the galaxy. Remarkable Hα filaments extend along the minor axis to a height of 3 kpc above and below the galactic plane.

Lynds and Sandage (1963) have observed the optical emission lines in M82 and found a velocity gradient of 1.5 km s^{-1} arcsec^{-1} along the filaments. Considering the inclination of the galactic plane, they argued that the velocity gradient must indicate an outflow of the gas from the galactic plane. The outflow velocity was suggested to be as high as about 1000 km s^{-1} at the edges of filaments, and all the matter in the filaments should have their origin near the galactic center 1.47×10^6 yr ago. Therefore, Lynds and Sandage (1963) have proposed that approximately 1.5 Myr ago there took place an extremely energetic explosion in the central region of M82. Burbidge et al. (1964) obtained a more precise velocity field and supported the explosion hypothesis of Lynds and Sandage (1963). The expansion velocity was determined to be 450 km s^{-1}.

However, observations of optical polarization of M82 showed that the electric vectors outside the galactic plane are parallel to concentric circles or ellipses (Solinger 1967; Elvius 1969; Solinger and Markert 1975; Bingham et al. 1976). Therefore, the polarized light in the halo may be originated near the galactic center and is scattered by dust particles in the halo. The detection of polarized Hα (Visvanathan and Sandage 1972) and [N II] λ6583 (Visvanathan 1974) emission supported this scattering model. If the scattering particles are moving away from the light source near the center, the observed light must show a redshift on *both sides* of the galactic plane according to the "moving mirror" effect, whereas the observations showed such redshift only on the northwestern side. Therefore, the explosion hypothesis advocated by Lynds and Sandage (1963) was not consistent with the scattering model, and alternative models have been proposed to explain the observed velocity field of M82 (Heckathorn 1972; Solinger et al. 1977). However, the optical light is affected by obscuration and is a mixture of the intrinsic emission and the scattered light, which makes the interpretation complicated. A direct measurement of the true velocity field in the galaxy is required.

The central region of M82 is a strong emitter from radio to X-ray wavelengths. The radio luminosity of M82 (7 Jy at 1.4 GHz) is one or two orders of magnitude higher than those of nearby ($\lesssim$10 Mpc) normal galaxies (e.g., Condon 1983). The infrared luminosity of $\simeq3.0\times10^{10}\,L_\odot$ (Telesco and Harper 1980) is also the largest in nearby galaxies. Radio observations suggest a high supernova rate, τ_{SN}, of 0.1–0.3 yr^{-1} (Kronberg and Wilkinson 1975; Rieke et al. 1980; Kronberg and Sramek 1985), which is one order of magnitude higher than τ_{SN} of our own Galaxy, M31, and M33 (Berkhuijsen 1984) in spite of the smaller linear size of the galaxy. Actually, at least 30 candidates of supernova remnants with luminosities 1–150 times that of Cas A have been identified in the inner 600 pc of M82 (Unger et al. 1984; Kronberg et al. 1985). The huge luminosity across the electromagnetic spectrum and the ex-

Table 1. Parameters of M82.

Center position (1950.0)[1]	R. A. = $09^h51^m43^s.9$
	Decl. = 69°55′01″
Classification	Irr II[2],[3]
	I0[4]
Systemic LSR velocity[5]	220 km s^{-1}
Distance[6]	3.25 Mpc
Position angle of the optical major axis[7]	65°
Inclination of the galactic plane[8]	81°37′ (90° is edge-on)

(1) The position of the 2.2-μm infrared peak (Rieke et al. 1980).
(2) Holmberg 1950, 1958.
(3) Sandage 1961.
(4) de Vaucouleurs and de Vaucouleurs 1964.
(5) Olofsson and Rydbeck 1984.
(6) Tammann and Sandage 1968.
(7) Nilson 1973.
(8) Lynds and Sandage 1963.

tremely high density of young supernovae suggest vigorous star formation in the galaxy.

The CO emission of M82 is also anomalously strong. The ratio of T_b(CO J=2–1)/T_b(CO J=1–0)$\simeq$3 (Sutton et al. 1983; Olofsson and Rydbeck 1984) suggests that much of the CO gas in M82 is optically thin, unlike typical molecular clouds in our Galaxy. The CO emission observed with the FCRAO 14-m telescope (Young and Scoville 1984) and the Bell Lab 7-m telescope (Stark and Carlson 1984) extends spatially out to at least 2′ from the plane of the galaxy beyond the optical disk. This extension of the CO emission is called the "molecular halo."

Although a number of CO observations of M82 have been made in the past 10 yr, the telescopes with angular resolutions of 30″–100″ were not able to resolve the CO distribution of the central region of the galaxy. We made new observations of the CO emission with an angular resolution of 16″ using the 45-m telescope of the Nobeyama Radio Observatory. We obtained a CO map of a region 1′.5 square in the center of the galaxy and were able to resolve the distribution of the molecular gas in the region of bursting star formation at the nucleus. Recent aperture synthesis observations of CO in M82 provided a higher resolution ($\sim$7″) and better positional accuracy ($\sim$1″) (Lo et al. 1987), whereas our observations with a filled-aperture telescope were sensitive even for the diffuse component of the molecular gas and the total bandwidth of the spectrometer (250 MHz) covered an entire velocity field of this nearly edge-on galaxy. In this paper, we report the results of the CO observations, discuss the structure and dynamics of the molecular gas, and propose a model for the behavior of gas in M82. Some parameters of M82 are given in table 1.

2. Observations

The observations were made in May and June 1984 and in March 1985 using the 45-m telescope of the Nobeyama Radio Observatory. The receiver frontend was a cooled mixer with an instantaneous bandwidth of 500 MHz. The system noise temperature (SSB) at 115 GHz including the atmospheric effect and the antenna ohmic loss

was 1000–1500 K (1984) or 600–800 K (1985). The spectra were taken with the 2048 channel wide-band acousto-optical spectrometer (AOS). The frequency resolution was 250 kHz corresponding to a velocity resolution of 0.65 km s^{-1} at the CO (J=1–0) frequency. The total bandwidth of an AOS (250 MHz) provided a velocity coverage of 650 km s^{-1}. The full half-power beamwidth (HPBW) at 115 GHz was 16″ which corresponds to 250 pc at the distance of M82 [3.25 Mpc; Tammann and Sandage (1968)]. The main-beam efficiency η_{mb} was measured to be 0.34 using the planet Venus.

The observations were made in the position switching mode. In one cycle of the switching observations, one "off" position was observed after observing three to five different "on" positions. At each position the signal was integrated for 20 s (on source) every cycle, and typically 30 cycles were repeated. The pointing was carefully calibrated by observing the SiO maser source T Cep. Each cycle always contained the center of M82 to check and calibrate the pointing and intensity scale. The rapidly rising rotation curve of the galaxy makes the CO profile sensitive to the pointing error. The absolute pointing accuracy was estimated to be better than ±4″ (peak value) for the observed points in the central 1′, and ±7″ for outside.

The calibration of the line intensity was made using an absorbing chopper in front of the receiver. The intensity scale is the antenna temperature, T_A^*, corrected for the atmospheric and antenna ohmic losses (Ulich and Haas 1976) but not for the beam efficiency. Moreover, the corrections of the relative intensity were made repeatedly by observing the CO emission at the center position of the galaxy. The probable error of the relative intensity scale was within ±20%. We also compared our brightness temperature in M82 with that obtained with other telescopes. Our CO line data were convolved with a Gaussian beam to a HPBW of the telescope with which the intensity scale was compared. Main-beam brightness temperatures, $T_{mb}=T_A^*/\eta_{mb}$ of reproduced CO spectrum at the center of M82 were 0.9, 1.0, and 1.2 times T_{mb} obtained with the OVRAO 10.4-m [HPBW=60″ (Sutton et al. 1983)], FCRAO 14-m [50″ (Young and Scovill 1984)], and Onsala 20-m [33″ (Olofsson and Rydbeck 1984)] telescope, respectively. Therefore, the error of the absolute intensity scale was within ±20%.

3. Distribution of the CO Gas

The ^{12}CO (J=1–0) emission from the central 1′.5×1′.5 (1400 pc) of M82 was mapped, with the map center at the 2.2-μm infrared peak of Rieke et al. (1980). In total, 69 positions were observed. The spacing was 7″.5 in the central 30″×30″ and 15″ in the outer part. Figure 1 shows the measured CO spectra. Vertical lines indicate the adopted systemic velocity, 220 km s^{-1}. The line profile at the center position itself has a clear symmetry about the systemic velocity. Also the change of line profiles along the major axis on both sides of the center shows a symmetry about the adopted center. These symmetries suggest that the 2.2-μm infrared peak is the center of rotation of the galaxy, and that it is very likely the nucleus of the galaxy within the pointing accuracy of a few arcseconds. In the line profiles at and around the center, weak (0.2 K) narrow (10 km s^{-1}) dips are noticed at $V_{LSR}\simeq$230 km s^{-1}. The dips are probably due to absorption by the CO gas either in the halo of M82 or in the H I bridge between

1987PASJ...39..685N

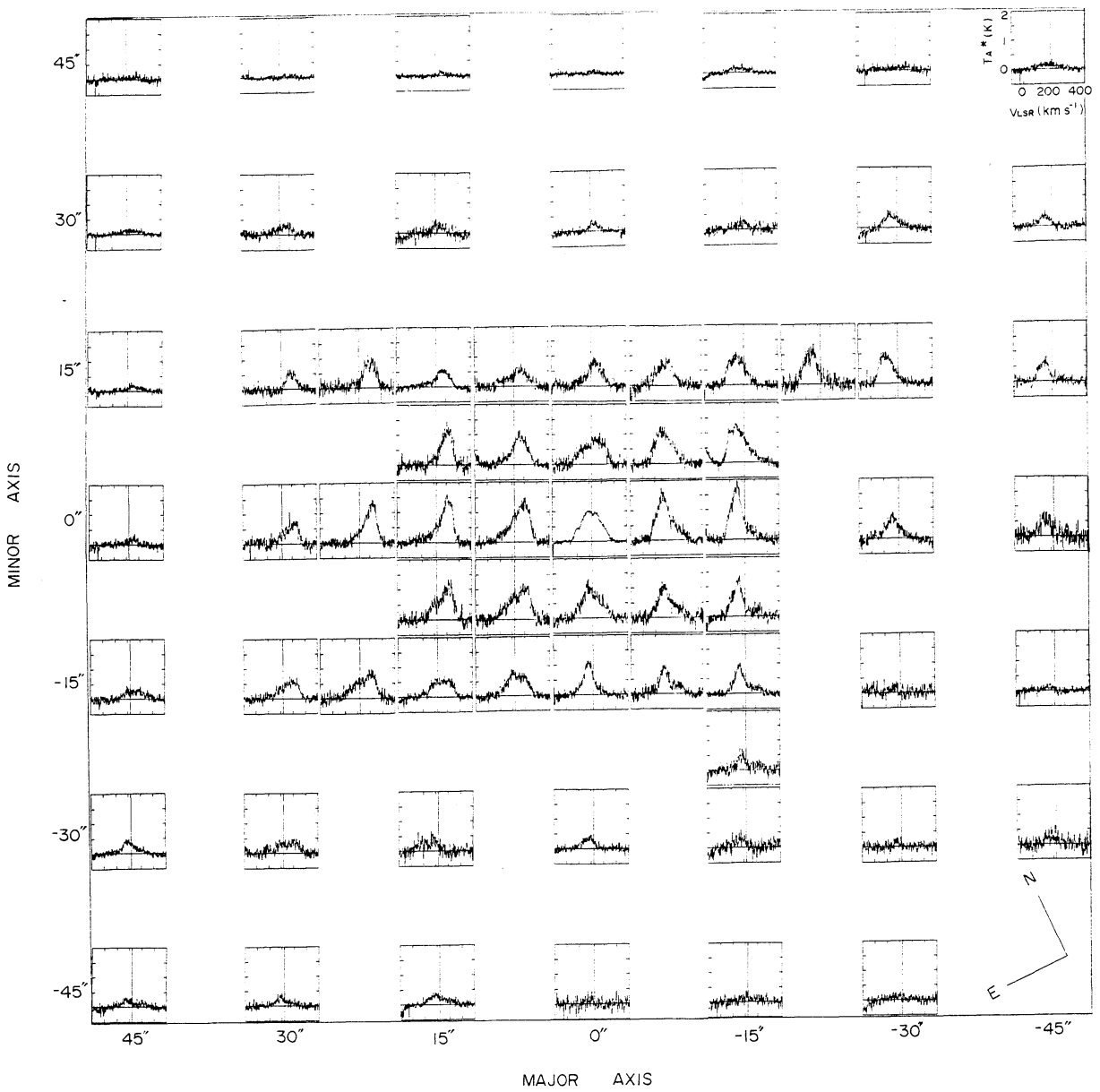

Fig. 1. The CO spectra for all of the observed points. The velocity resolution is 2.6 km s^{-1}. The vertical lines indicate the adopted systemic [illegible] of M82, 220 km s^{-1}. The intensity scale is the antenna temperature corrected for the atomospheric and antenna ohmic losses, but

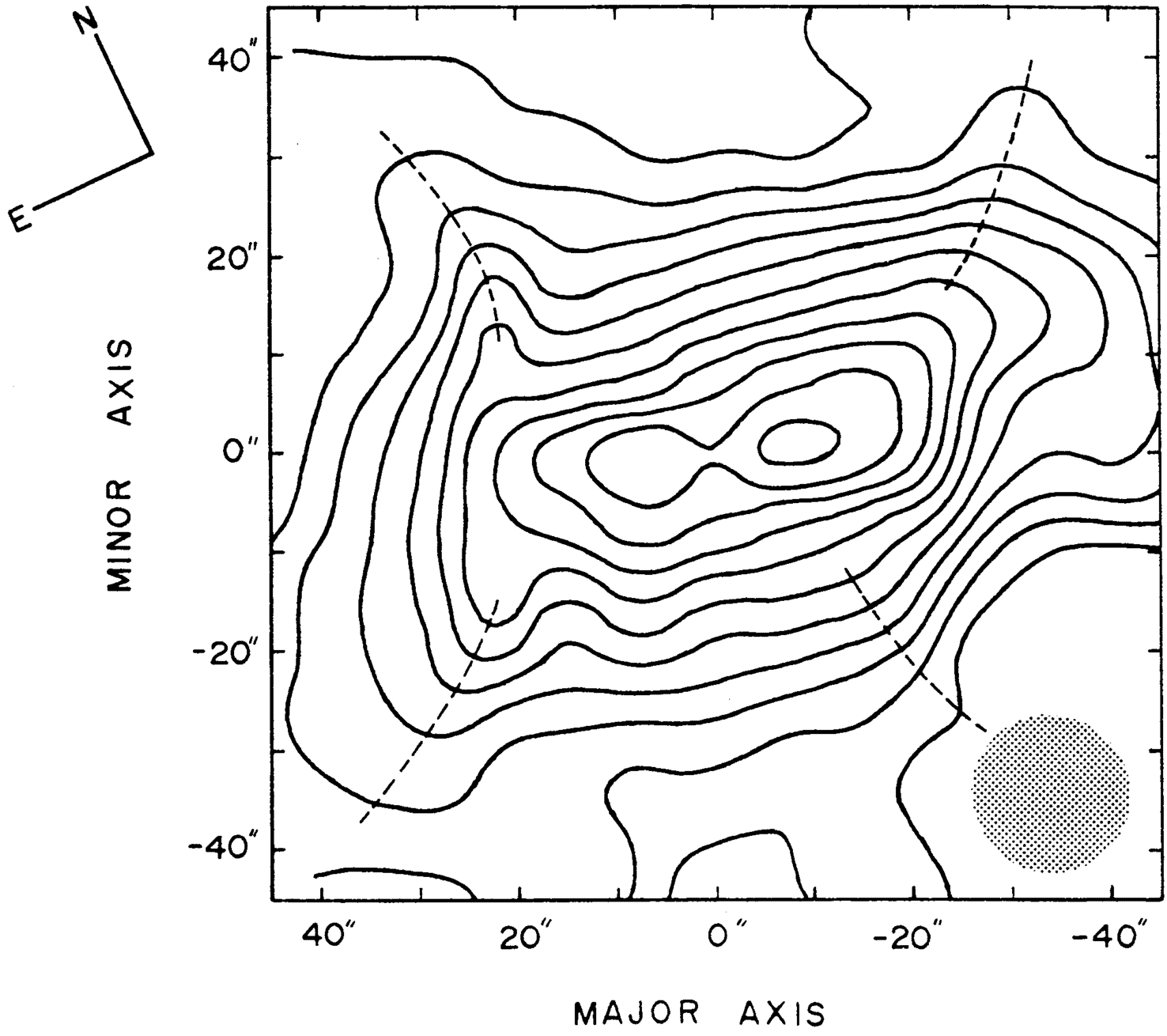

Fig. 2. The map of the integrated intensity of the CO emission, $I_{CO}=\int T_A^*(CO)dv$, with the integration range of 0–400 km s^{-1}. The lowest contour level and the contour interval are 20 K km s^{-1}. Dotted lines indicate ridges of the CO distribution which is elongated from the galactic disk toward the halo. The telescope beam (HPBW=16″) is shown by a hatched circle.

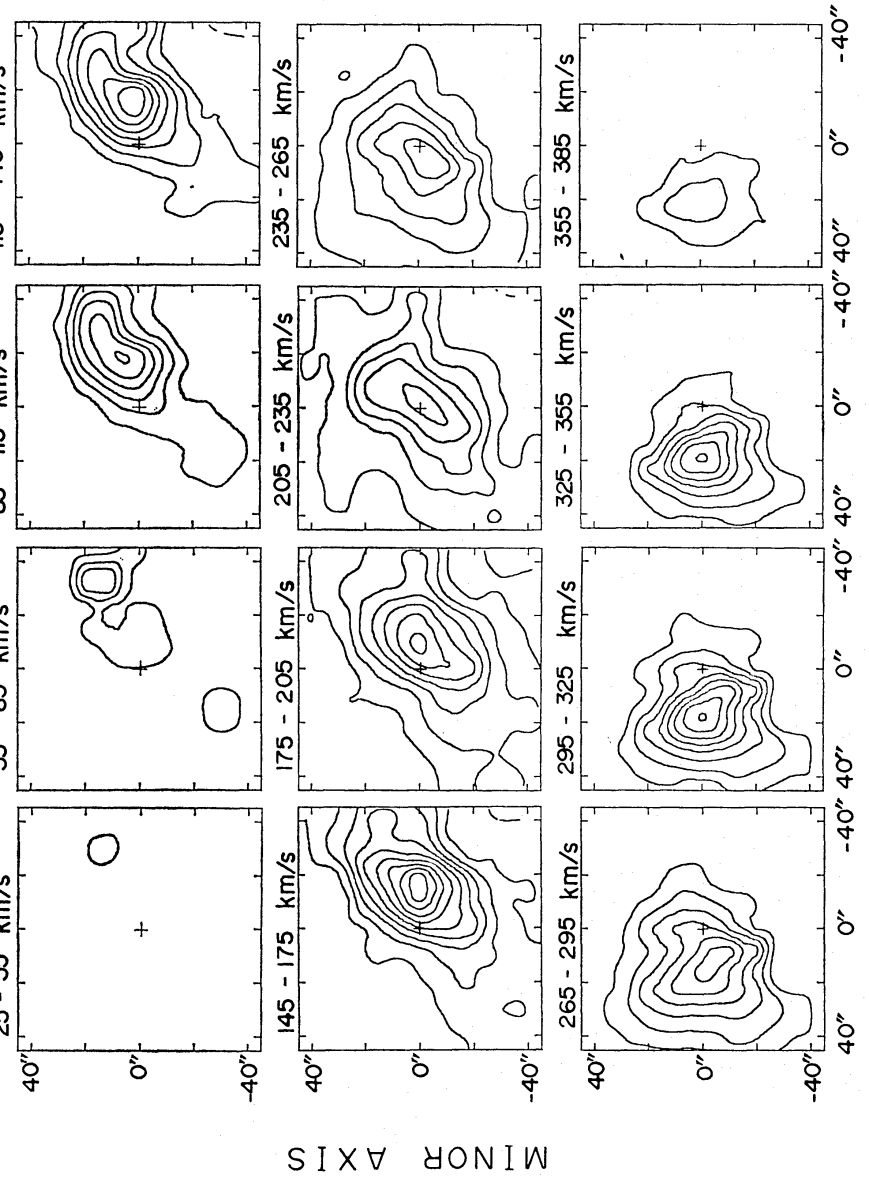

Fig. 3. Maps of the integrated intensity I_{CO} with the velocity width of 30 km s^{-1}. The velocity range is denoted at the top of each map. The lowest contour level and the contour interval are 5 K km s^{-1}. The cross in each map indicates the position of the galactic nucleus.

M81 and M82 (Nakai et al. 1986).

In this section, we present the distribution of the CO line intensity and estimate the mass of the molecular gas in the observed region. Next, we obtain a three-dimensional distribution of the density of the molecular gas based on an axisymmetric model. We compare the results with other data such as infrared, radio continuum, and X-ray emissions.

3.1. *Intensity Distribution*

Figure 2 shows a map of the integrated intensity $I_{CO} \equiv \int T_A^*(CO) dv$ of the CO line emission. The large-scale distribution of I_{CO} shows a rectangular shape with its major axis inclined by about 17° from the optical major axis at p.a.=82°. The extention of the CO emission (FWHM) is about 32″ (≃500 pc) along the minor axis and 55″ (≃910 pc) along the major axis of the CO distribution. The characteristic feature in the figure is the four ridges of the emission elongating toward the halo of the galaxy (dotted lines). Figure 3 shows maps of the intensity integrated with the velocity width of 30 km s^{-1}. The maps with the velocity of 145–175 km s^{-1}, 265–295 km s^{-1}, and 295–325 km s^{-1} also show clearly the structures extending almost perpendicular to the galactic plane.

The intensity distribution in the central region in figure 2 shows two peaks at both sides of the nucleus, or at $(X, Y)=(+6'', -1'')$ and $(-9'', +1'')$. The emission is weaker at the nuclear position than at the two peaks. The positions of the two peaks are about 100–150 pc away from the nucleus along the major axis and coincide with the sites of current star formation (see subsection 3.4). The double structure of the CO intensity was also found with the Owens Valley millimeter-wave interferometer (Lo et al. 1987), although the distance between the two maxima is larger than our result.

The elongated main body including the two peaks is inclined by about 7°–10° from the optical major axis which is at p.a.=65°. The inclinations of the major axis determined from the infrared emission, the radio continuum emission, and the H I absorption are also about 7°–13° relative to the optical major axis (p. 699, figure 8). The true position angle of the major axis of the inner part of the galaxy is, consequently, p.a.=75°±3° rather than 65°. This is mainly because the optical feature of the galaxy is affected badly by the internal absorption and shows only the structure of the side nearer to the observer. The discrepancy between the position angles of the optical (outer side) major axis and radio or infrared (inner disk) major axis is probably due to the warp of the galactic plane.

3.2. *Mass*

We estimate the mass of the molecular gas in the observed area. In the central region of M82, the ^{12}CO emission is suggested to be optically thin as discussed in the following. If the optical depth of ^{12}CO emission is very large ($\gg 1$), the ratio of the brightness temperature of the CO ($J=2$–1) line to that of CO ($J=1$–0) line emission is about unity as usually seen in molecular clouds in our Galaxy (e.g.,Phillips and Huggins 1977) and external galaxies (e. g., Knapp et al. 1980; Lo et al. 1980). If the CO gas is in an optically thin limit, on the other hand, the ratio of the CO ($J=2$–1)

to CO (J=1–0) brightness temperature is $4\exp(-5.5/T_{ex})$ and is about 3.5 for the excitation temperature T_{ex} of 40 K adopted below. Knapp et al. (1980) found the ratio to be 3.5 ± 1.2 in M82. Recently Olofsson and Rydbeck (1984) obtained the ratio of 2.4 by comparing their CO (J=1–0) data and CO (J=2–1) data observed by Sutton et al. (1983), where the beam sizes for both observations were almost the same. The ratio 2.4 of the brightness temperature and the excitation temperature of 40 K indicate $\simeq0.35$ as the optical depth of the J=1–0 transition. Furthermore, the ratio of T_A* (^{12}CO J=1–0)/T_A*(^{13}CO J=1–0) in M82 is 30 ± 8 (Stark and Carlson 1984) or 21 ± 2 (Young and Scoville 1984), which is considerably higher than the values 5–10 in the galactic molecular clouds and in other galaxies. These results tend to support the optically thin hypothesis of the ^{12}CO emission. We hereafter assume that the ^{12}CO (J=1–0) emission is optically thin in M82.

It is now possible to estimate the mass of the molecular gas from the integrated intensity in figure 2. We assume that CO molecules are in a rotational equilibrium with hydrogen molecules and hence the excitation temperature T_{ex} of CO molecules is equal to the kinetic temperature T_k of hydrogen molecules. We also suppose that the hydrogen molecules are close to thermal equilibrium with dust grains. Various temperatures have been reported for dust in M82 [26 K (Harper and Low 1973), 45 K (Telesco and Harper 1980; Jaffe et al. 1984), and 49 K (Rickard and Harvey 1984)]. We will adopt $T_{ex}\simeq40$ K for the CO gas in the following calculations.

It is more difficult to estimate the value of the abundance ratio [CO]/[H_2] in M82. There were neither direct estimates of [CO]/[H_2] nor determinations of chemical abundances, for example, using optical emission lines from H II regions or supernova remnants in the galaxy. However, the [HCN]/[CO] and [HCO^+]/[CO] abundance ratios in M82 are roughly in the range of the galactic values, if these emissions are optically thin (Rickard et al. 1977; Stark and Wolff 1979). The ratio of [OH]/[H I] is in agreement with the value in our Galaxy (Weliachew et al. 1984). We here assume simply that the abundance ratio [CO]/[H_2] in M82 is not so different from that in our Galaxy. A value of $(1\text{–}10)\times10^{-5}$ has been derived for the [CO]/[H_2] ratio in our Galaxy (e.g., Dickman 1975; Leung and Liszt 1976; Frerking et al. 1982). We adopt [CO]/[H_2]$\simeq5\times10^{-5}$ for M82.

Under these assumptions, the peak column density and the total mass of the molecular hydrogen in the observed area (1400 pc$\times$1400 pc) are estimated to be $N(H_2)_{peak}\simeq2.3\times10^{22}$ cm^{-2} and $M(H_2)\simeq1.1\times10^8\,M_\odot$, respectively. The mass of the atomic hydrogen in this region is M(H I)$\simeq0.5\times10^8\,M_\odot$ as estimated from the H I data of Crutcher et al. (1978). Hence the molecular to atomic hydrogen ratio is $M(H_2)/M$(H I)$\simeq2.2$. The dynamical mass of M82 can be derived from the rotation curve in subsection 4.1. The derived mass, M(dyn), within r=45″ is from $1.1\times10^9\,M_\odot$ [a flat disk distribution (Nordsieck 1973)] to $1.2\times10^9\,M_\odot$ (a purely spherical distribution). Thus, the ratios of the gaseous mass to the dynamical mass are $M(H_2)/M$(dyn) $\simeq0.10$ and $[M(H_2)+M$(H I)$+M$(H II)$]/M$(dyn)$\simeq0.20$. In our Galaxy, the empirical relation of $N(H_2)\simeq(3\text{–}5)\times10^{20}\int T_A$*(CO)$dv$ cm^{-2} for a telescope with $\eta_{mb}\simeq0.6$ has been obtained for a large sample of optically thick clouds in our Galaxy (e.g., Young and Scoville 1982; Liszt 1982; Sanders et al. 1984). If we apply this relation to our data of M82 adopting η_{mb}=0.34 for the 45-m telescope, the mass of the molecular gas is

Table 2. Masses in the center of M82.

Material	Mass ($M_\odot$)	Diameter[a] (pc)
Molecular hydrogen (H_2)[b]	1.1×10^8	1400
Atomic hydrogen (H I)[c]	5×10^7	1400
Ionized gas (H II)[d]	7×10^7	1100
Dust[e]	5×10^5	500
Total mass[f]	$(1.1\text{–}1.2)\times10^9$	1400

[a] Diameters of observed areas within which masses are estimated.
[b] Obtained from this work, assuming a low optical depth, $T_{ex}\simeq40$ K, and $[CO]/[H_2]\simeq5\times10^{-5}$.
[c] Obtained from the H I data of Crutcher et al. (1978).
[d] Willner et al. 1977.
[e] Telesco and Harper 1980.
[f] Dynamical mass calculated from the CO rotation curve. The lower and upper values are given by a flat-disk model and a purely spherical model, respectively.

$(1.1\text{–}1.9)\times10^9\ M_\odot$ which exceeds the dynamical, hence, the total mass. This fact confirms that the optical depth in M82 is smaller than that of the clouds in our Galaxy. Various masses in the center of the galaxy are summarized in table 2.

3.3. *Density Distribution Based on an Axisymmetric Model*

The intensity distribution of the CO gas in figure 2 is fairly symmetric about the minor axis. We may estimate a three-dimensional density distribution of the molecular gas in M82 based on an axisymmetric model. We define the plane of the gas disk inclined by 10° from the optical major axis (subsection 3.1). The axis of the rotation is taken as the line through the nucleus perpendicular to this plane. Distances from the axis of the rotation and from the disk plane are specified by r and z, respectively. We follow the procedure of Watanabe et al. (1982) to construct an axisymmetric model. First the galaxy is divided into twelve slabs with a thickness of $\Delta z=7''.5$ (observing grid spacing) perpendicular to the rotation axis; then, each slab is divided into rings with a width of $\Delta r=7''.5$ and a uniform number density n. We neglect the inclination of the disk plane to the line of sight (probably $<15°$; section 5) for simplicity. The volume number density n of the molecular hydrogen in each ring is determined to reproduce the column density derived from the observed CO intensity (figure 2). The values of n are obtained from the outermost ring to the innermost ring, where we assume $n(H_2)\simeq0$ at $r>2'.5$, $z=0''$ and at $r>2'$, $z=\pm45''$ according to the results of CO observations of a larger field (Olofsson and Rydbeck 1984; Young and Scoville 1984). The conversion of the CO integrated intensity to the H_2 column density is performed as described in the preceding subsection.

Figure 4 shows the resulting distribution of the volume number density, where the first contour level and the contour interval are 1 H_2 cm^{-3}. The error is larger in the inner rings and is about ±2 H_2 cm^{-3} at $r=0$. Most of the H_2 mass ($\simeq0.9\times10^8 M_\odot$) is distributed within $r<500$ pc and the mean surface density projected on the galactic plane in this area is $\simeq130\ M_\odot$ pc^{-2}. These mass and the surface density are about a half of those in our Galaxy within $r<500$ pc ($2.38\times10^8\ M_\odot$ and $303\ M_\odot$ pc^{-2}; Sanders et al. 1984).

The dense region ($n\geq6$ H_2 cm^{-3}) of the molecular gas exists at 80–400 pc (centered

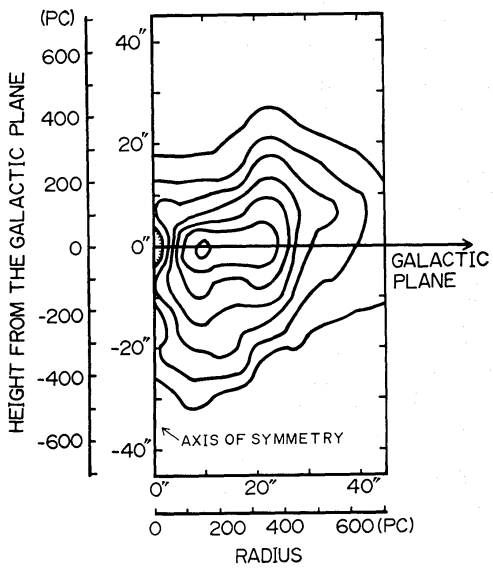

Fig. 4. The volume number density of hydrogen molecules calculated with an axisymmetric model based on the CO map of figure 1. The coordinates are (r, z), where the r axis is in the galactic plane and the z axis perpendicular to it through the nucleus. The lowest contour level and the contour interval are 1 H_2 cm^{-3}.

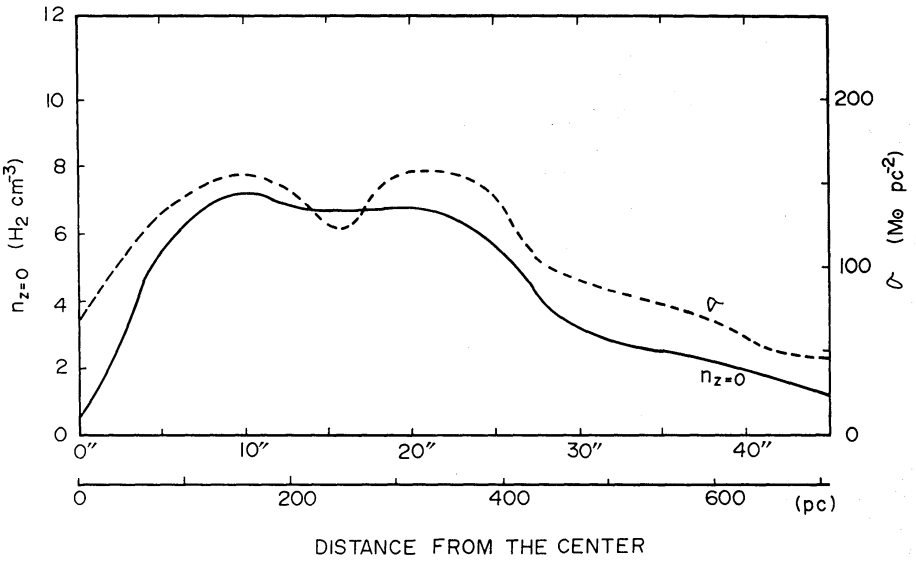

Fig. 5. Radial distributions of the volume number density $n_{z=0}$ (H_2 cm^{-3}) at the galactic plane ($z=0$) and the surface density σ ($M_\odot$ pc^{-2}) of the molecular hydrogen projected to the galactic plane.

on about 200 pc) from the center on the galactic plane and shows a ring structure (figure 5). The mass of the molecular gas in this ring (toroid) is $\simeq 3\times 10^7\ M_\odot$ within $z=\pm 100$ pc. This molecular ring, which we call hereafter the "200-pc ring," corresponds to an active site of star formation as mentioned in the next subsection. Inside the 200-pc ring we find clearly a "central hole" of the molecular gas where the density is less than 2 H_2 cm^{-3}. The ring structure, which is based on an axisymmetric model, is of course not a unique model to reproduce the observed distribution of the CO

column density. However, the axisymmetric distribution is the simplest hypothesis and at least the depletion of the molecular gas in the nucleus is an undeniable fact even in other models. Such a nuclear ring of the molecular gas has been observed for the barred spiral galaxy NGC 1097 (Gérin et al. 1987).

Another prominent feature revealed in figure 4 is a spurlike structure which emerges almost perpendicularly to the galactic disk from $(r, z) \simeq (350$ pc, 100 pc) toward the northern halo ($z>0$). Inside the spur, the density of the molecular gas is low and a cavity wall or a hollow cylinder with a radius of $\simeq 400$ pc is formed. The spurlike feature at the southern side ($z<0$) of the galactic plane also is elongated from $(r, z) \simeq (150$ pc, -100 pc) to (150 pc, -500 pc) – (400 pc, -300 pc). The density contrast between the southern spur and the inside cavity is smaller than that in the northern side.

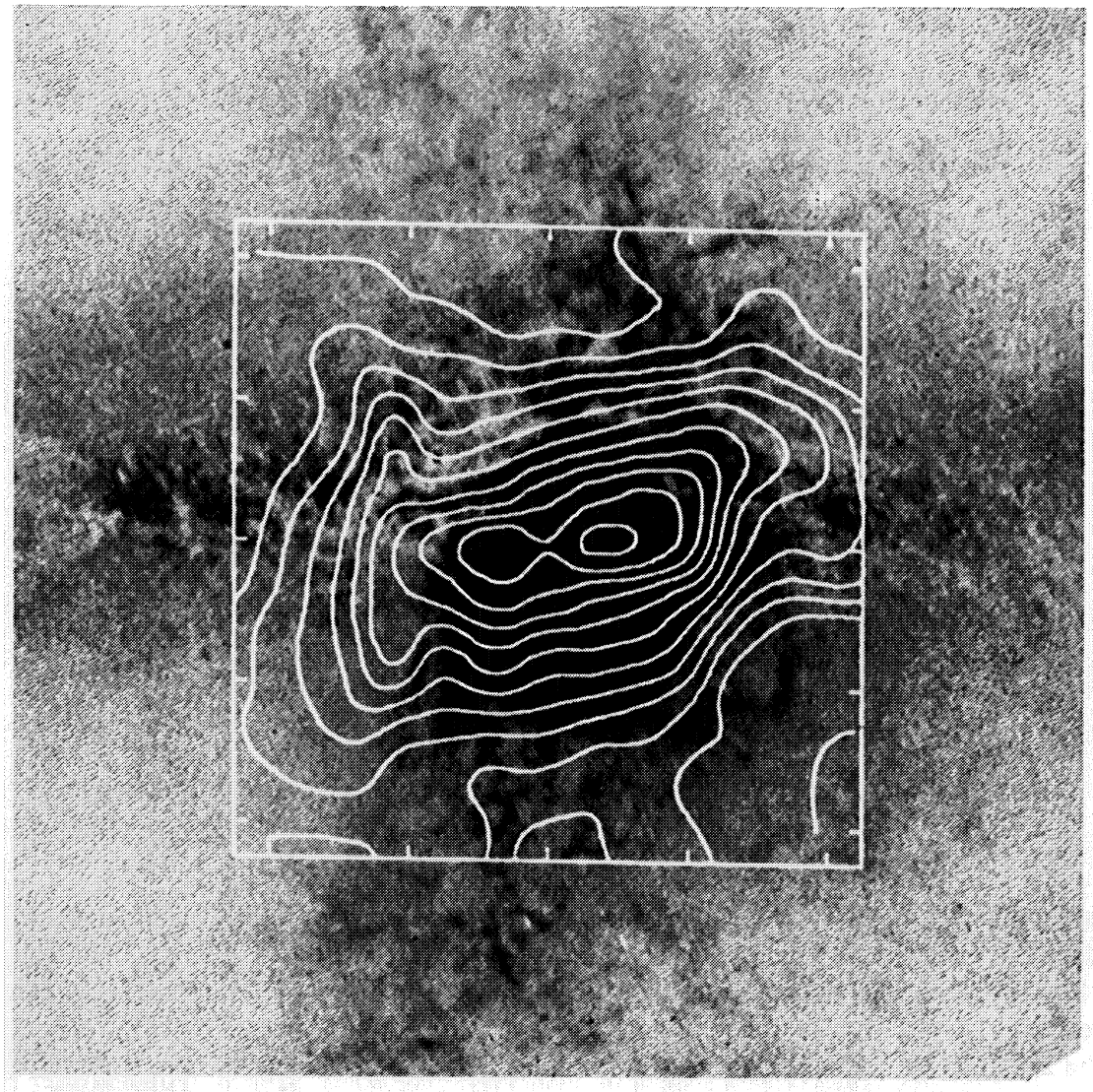

Fig. 6. Superposition of the CO intensity map (figure 2) on the Hα photograph of McCarthy et al. (1987), where the continuum component was subtracted from the original Hα plate.

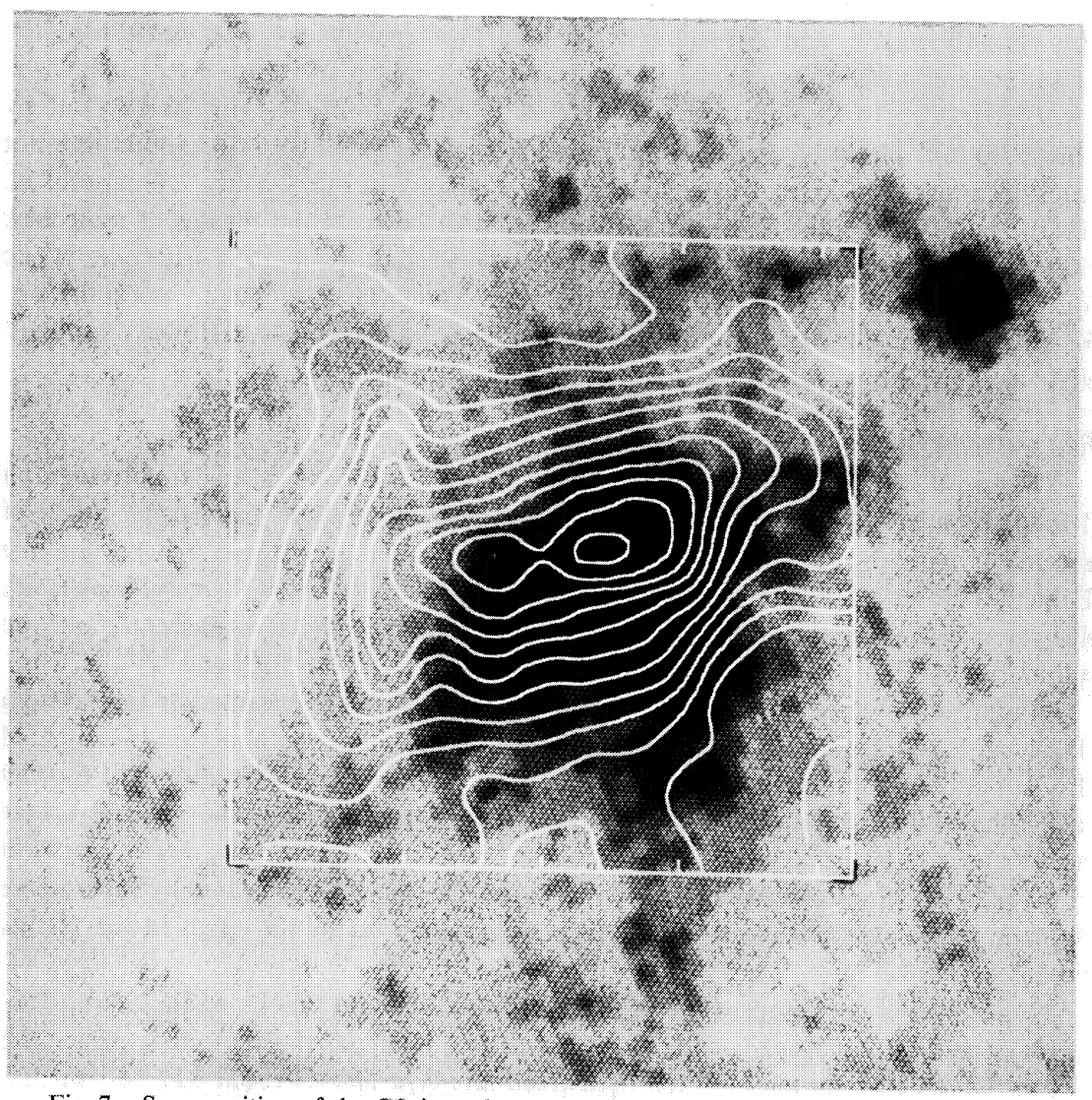

Fig. 7. Superposition of the CO intensity map (figure 2) on the X-ray image (gray scale) of Watson et al. (1984).

3.4. *Size and Mass of Molecular Clouds*

We can estimate the size and the mass of molecular clouds in M82 from the volume and surface filling factors f_V and f_S. We consider spherical clouds with a diameter a and a density $n(H_2)$. The diameter may be obtained as $a \simeq 3 f_V l/(2 f_S)$, where l is the line-of-sight length of the region, in which molecular clouds are distributed, and is about 1000 pc (see figure 4). The volume number density in figure 4 does not exceed $8 H_2$ cm^{-3}. This value is lower by three orders of magnitude than the density $n(H_2)$ required to collisionally thermalize the rotational transition of CO. Therefore, the volume filling factor is of the order $n(H_2)^{-1} \simeq 10^{-3}$. The surface filling factor is $f_S \simeq T_A^*/\{T_{ex}[1-\exp(-\tau)]\eta_{mb}\} \simeq 0.25$, where $T_A^* \simeq 1$ K around the center (figure 1), $T_{ex} \simeq 40$ K, $\tau \simeq 0.35$ (subsection 3.2), and $\eta_{mb} \simeq 0.34$. Hence the diameter of molecular clouds is $a \simeq 6\,[n(H_2)/10^3\ cm^{-3}]^{-1}$ pc and the mass $M \simeq 6 \times 10^3 [n(H_2)/10^3\ cm^{-3}]^{-2}\ M_\odot$.

The numbers of molecular clouds in the observed area and in the 200-pc ring are $2\times 10^4[n(H_2)/10^3\ cm^{-3}]^2$ and $5\times 10^3[n(H_2)/10^3\ cm^{-3}]^2$, respectively. The central region of M82 seems to be dominated not by such giant molecular clouds [$a\simeq 40$ pc, $M\simeq 5\times 10^5\ M_\odot$, $T_k\simeq 10$ K (Solomon and Sanders 1980)] as found in our Galaxy but by hot ($\simeq 40$ K), relatively small ($\simeq 6$ pc), and low-mass ($\simeq 6\times 10^3\ M_\odot$) clouds like hot cores in molecular clouds associated with H II regions in our Galaxy. Knapp et al. (1980) and Olofsson and Rydbeck (1984) estimated the sizes and masses of molecular clouds in M82 from the optical depth of CO and found $a\simeq 0.1[n(H_2)/10^4\ cm^{-3}]^{-1}$ pc for optically thin CO ($J=2$–1) clouds and $a\simeq 0.6[n(H_2)/10^4\ cm^{-3}]^{-1}$ pc and $M\simeq 50[n(H_2)/10^4\ cm^{-3}]^{-2}\ M_\odot$ for optically thin CO ($J=1$–0) clouds. If we adopt $10^4\ cm^{-3}$ as $n(H_2)$, our results are consistent with their results.

3.5. *Comparison with Other Data*

Figure 6 shows a superposition of the CO intensity map on an Hα photograph (McCarthy et al. 1987). The Hα filaments extend toward the halo at an angle of about 80° with respect to the optical major axis, and the northwestern part of the filaments shows a fan-shape structure with several spurs. The CO spurs which are elongated toward the halo are distributed just outside of the Hα filaments, and the cylinder of the molecular gas in figure 4 seems to wrap the Hα filaments.

Figure 7 shows the CO map superposed on an X-ray image obtained by the Einstein Observatory (Watson et al. 1984). The distribution of the X-ray emission is elongated almost parallel to the minor axis of the galaxy and is found inside the ridges of the CO gas. The X-ray emission is slightly asymmetric with respect to the galactic center and is shifted toward the southwest. This is probably because the X-ray emission from the halo is due to thermal emission from the hot gas which is heated by supernovae (Watson et al. 1984), and supernova events are active in the SW than in the NE as discussed below.

Figure 8 shows a map of the 2.2-μm infrared emission (Rieke et al. 1980). The 2.2-μm emission is sharply peaked at the "central hole" of the molecular gas. The flux at 2.2 μm is dominated by the light from late-type stars: About 82% of the 2.2-μm flux in M82 comes from red giants and supergiants with the masses of 6–10 $M_\odot$, according to the star burst model of Rieke et al. (1980). The gas in the nucleus was perhaps consumed in the formation of stars or was blown off toward the halo (section 5).

Figure 8 also shows maps of the 10-μm infrared emission (Rieke et al. 1980) and the 1667-MHz radio continuum emission [observed by F. N. Owen and B. E. Turner and referred by Kronberg et al. (1981)]. Peaks of these emissions at about 10″ southwest of the nucleus coincide with that of the CO emission. Especially, a powerful [luminosity >100 times that of Cas A; e.g., Kronberg and Biermann (1983)] and very compact [0.3 pc; Wilkinson and de Bruyn (1984)] radio source 41.9+58 is just on the CO peak. The northeastern peak of the CO emission also corresponds to a peak of the radio continuum and a weak peak of the 10-μm emission. The 10-μm flux is predominantly thermal reradiation from heated dust in ionized regions associated with massive stars (e.g., Scoville et al. 1983). The radio continuum emission of M82 at 1667 MHz is of the nonthermal origin and its large fraction could be attributed to

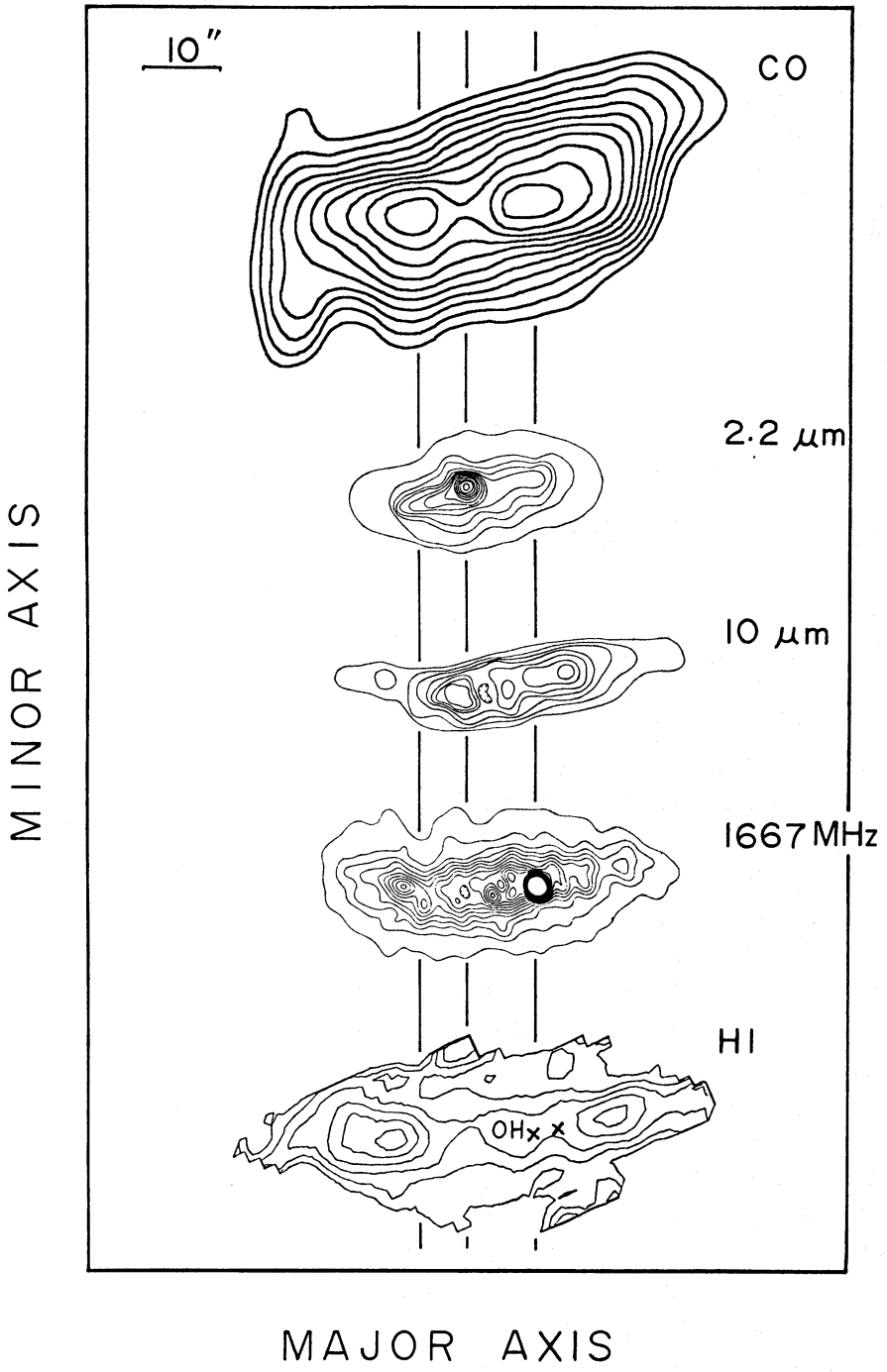

Fig. 8. Comparisons of the CO distribution in the nuclear region (with a 16″ beam) with distributions of the 2.2-μm and 10-μm infrared emission (2″.5; Rieke et al. 1980), the 1667-MHz radio continuum emission (2″.2; Kronberg et al. 1981), and optical depth of the atomic hydrogen with positions of two OH masers (crosses) (6″.0 × 3″.8; Weliachew et al. 1984). The outermost contour and contour interval in the CO map are 120 and 10 K km s^{-1}, respectively. The contour interval at 2.2 μm is 7×10^{-19} W m^{-2} Hz^{-1} sr^{-1} and at 10 μm is 2.2×10^{-18} W m^{-2} Hz^{-1} sr^{-1}. In the map at 1667 MHz, the peak surface brightness is 390 mJy beam^{-1}, and contours are drawn at intervals of 2.5% of peak brightness up to 50%. In the H I map, the contour increment is 0.03 in optical depth which corresponds to 1.7×10^{21} cm^{-2} column density of the H I gas for an excitation temperature 100 K. Vertical lines indicate positions of the nucleus (2.2-μm peak) and two peaks of the CO distribution.

supernova remnants (Rieke et al. 1980). In M82, consequently, the current site of the formation of massive stars and supernovae coincides with the 200-pc ring of the molecular gas.

Observations of H I absorption using the VLA show two peaks (figure 8) which have suggested a rotating H I ring (Weliachew et al. 1984). The intense peaks are apparently located slightly outside the CO peaks. Recent interferometer observations of CO (Lo et al. 1987) showed a larger distance between the two peaks of CO than that of ours and their peak positions are in agreement with those of H I. Although the reason for the discrepancy between two results of ours and Lo et al. (1987) is not so clear, the smaller distance between CO peaks of our data could be attributed to the larger beam size of the 45-m telescope. The integrated intensity at NE positions from the galactic center contains the emission at SW positions with the foot of the Gaussian beam, and vice versa, so that the maxima of the integrated intensity might move toward the center. The discrepancy is not due to the pointing of our observations, because the CO spectra at the central five positions along the major axis in figure 1 were simultaneously obtained and the relative pointing between the five positions is accurate.

We here discuss possible origins of the molecular ring. Sanders (1979) and Fukunaga (1983, 1984) have explained the 5-kpc and 300-pc molecular rings in our Galaxy in terms of shear viscosity by large-scale cloud-cloud interactions. The angular momenta of molecular clouds in a region of differential rotation are transferred outward and are lost in the inner part of the Galaxy. As a consequence, molecular clouds fall toward the rotational center and accumulate in the transition region between the outer region of differential rotation and the inner region of rigid rotation. In M82 such a mechanism might occur for the formation of the molecular ring, because the position of a density maximum of the molecular gas is almost coincident with that of a velocity maximum in the rotation curve (figures 9 and 10).

Another possibility is that M82 might have a bar or an oval structure in the center. It is observationally known that inner rings are most common among the barred galaxies (e.g., de Vaucouleurs and Buta 1980). Particle simulations have shown that oval or barlike distributions of potential fields can form rings of gas near the inner Lindblad resonance (e.g., Schwarz 1984; Combes and Gerin 1985). Therefore, the molecular ring in M82 might be due to a bar potential, although it is difficult to know whether M82 has a bar, because the galaxy is nearly edge-on.

Finally, probably the most promising mechanism is that of the ring formation by a shock compression of the gas caused by the supernova shockwaves and mass outflow from stars in the starburst region at the center. The gas in the nuclear region was perhaps blown off toward the halo.

4. Kinematical Structure

4.1. Rotation Curve in the Inner Galaxy

Figure 9a shows a position–velocity diagram along the optical major axis, which clearly indicates the rotation of the galaxy. Figure 10 shows the rotation curve of the galaxy at $|r|<45''$ (710 pc at the distance of 3.25 Mpc). Rotational velocities have

been measured at velocities where line profiles of the CO emission are sharply decreasing. The rotation curve near the nucleus rapidly rises up to $V_{\rm rel}\simeq 120$ km s^{-1} and $V_{\rm rel}\simeq 130$ km s^{-1} above and below the adopted systemic velocity ($V_{\rm sys}=220$ km s^{-1}), where $V_{\rm rel}=|V_{\rm LSR}-V_{\rm sys}|$ is a relative velocity to the systemic velocity. The peak velocities are much smaller than those of our Galaxy [$\simeq 260$ km s^{-1} (Burton and Gordon 1978)]

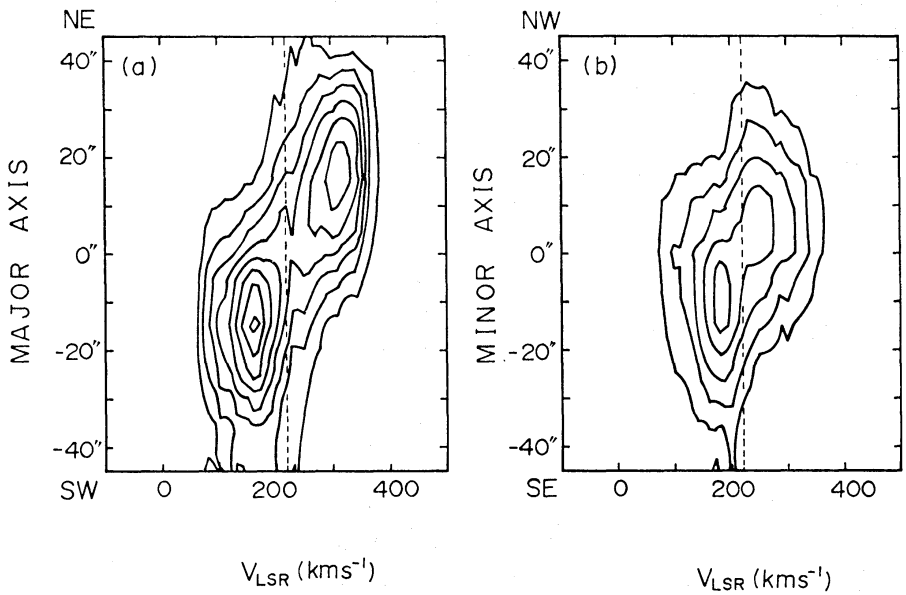

Fig. 9. Position–velocity diagrams of the CO line emission along the major axis (a) and the minor axis (b). The contour intervals are 0.2 K. The dotted lines indicate the adopted systemic velocity, 220 km s^{-1}.

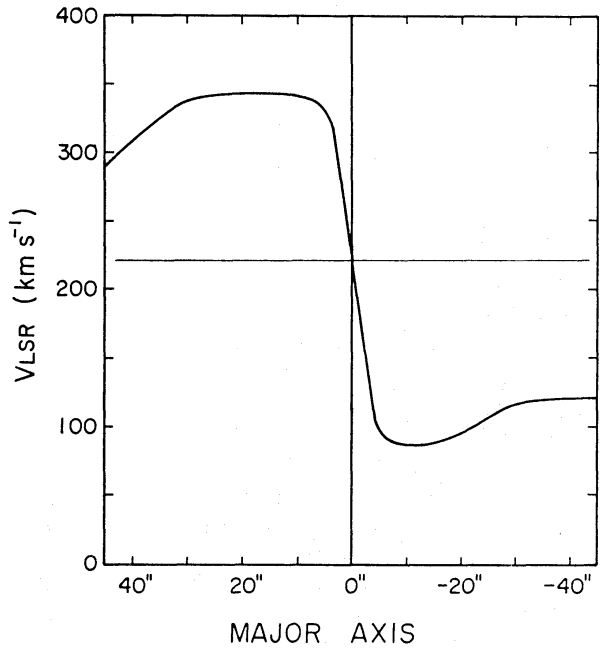

Fig. 10. Rotation curve at $|r|<45''$. Rotational velocities have been measured at velocities where the CO emission velocity is sharply decreasing.

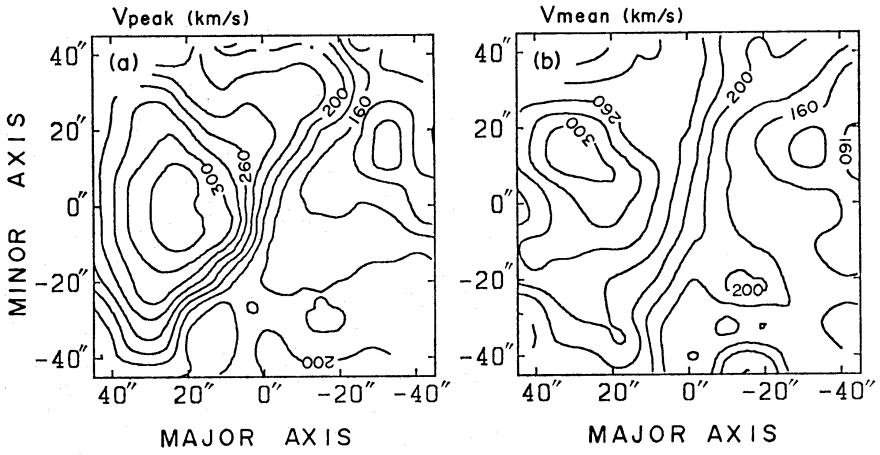

Fig. 11. Isovelocity curves made from the peak velocities (a), and from the intensity-weighted mean velocities (b). The unit of contour numbers is km s^{-1}. The velocity gradient along the minor axis is clearly seen.

and M31 [270 km s^{-1} (Rubin and Ford 1970)]. This indicates that the mass of the central region ($r<500$ pc) of M82, $1\times10^9\ M_\odot$, is smaller than those of our Galaxy [$8.3\times10^9\ M_\odot$ (Oort 1977)] and of M31 [$4\times10^9\ M_\odot$ (Rubin and Ford 1970)]. It is impossible to derive the rotation curve at $|r|>45''$, because asymmetry of the CO velocity curve becomes prominent, probably, due to a tidal interaction with M81 (Olofsson and Rydbeck 1984).

4.2. *Velocity Gradient along the Minor Axis*

Figure 9b shows a position–velocity diagram along the optical minor axis. Figures 11a and b show isovelocity maps constructed from peak velocities and intensity-weighted mean velocities, respectively. A velocity gradient along the minor axis is apparent. The relative velocity $V_{\rm rel}$ to the systemic velocity rapidly increases with the height from the galactic plane and has maximum velocities of $V_{\rm rel}=30$ km s^{-1} at the NW side and of 40 km s^{-1} at the SE side. The velocity gradient cannot be produced by pure circular rotation of the galactic disk, suggesting some opposite motions of molecular gas above and below the galactic plane.

The velocity field of the CO emission in figure 11 is slightly different from that of the Hα emission (Heckathorn 1972), which shows nearly a constant velocity in the inner region of $<25''$, and red- and blue-shifted velocities over 25″ at the NW and SE sides of the plane, respectively. The difference could be caused by a fact that the optical measurement gives information only for the near side of the galaxy due to the extinction by dust, while at the radio wavelength the whole galaxy can be seen. The velocity field of the CO emission is important to investigate the true motion of gas. An interpretation of the velocity shifts along the minor axis will be given in the next section.

5. An Expanding Cylinder Model

We summarize the observational facts on which the model is based. (i) The spurlike structures seen in the CO map extend out to $\geq\pm30''$ (±500 pc) above

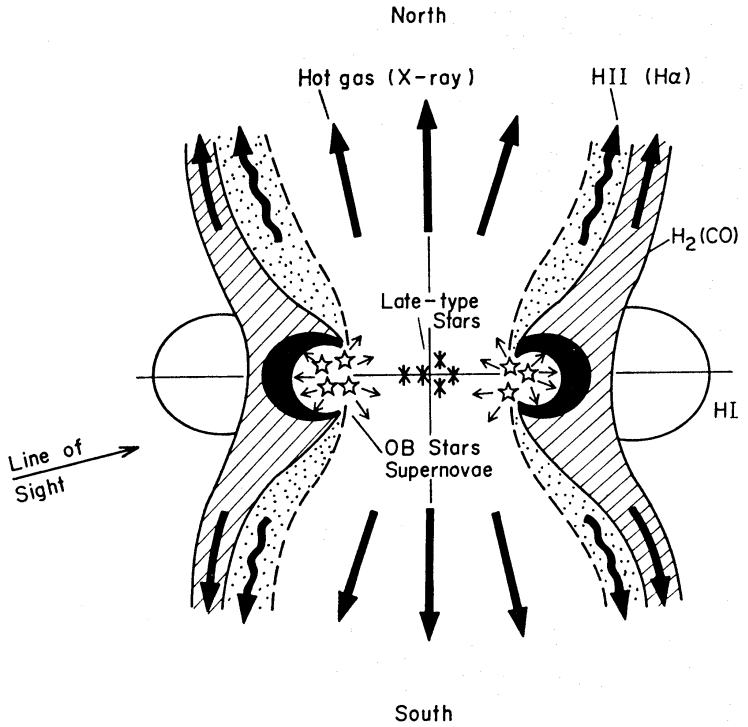

Fig. 12. A schematic view of flowing-out molecular gas, ionized gas (Hα filaments), and hot plasma (X-ray). The expanding velocity of the molecular gas is estimated to be 100–500 km s^{-1} for the inclination angle of 70°–85° (90° is edge-on).

and below the plane (figure 2). They may be tangential walls of a hollow cylinder of the molecular gas almost perpendicular to the disk plane (figure 4). The molecular spurs are well related with the distributions of the Hα filaments and the diffuse X-ray halo; the molecular spurs lie just outside the hot gases extending along the minor axis from the nuclear region (figures 6 and 7). Such a cavity wall in the halo is also seen in the H I gas (Cottrell 1977). (ii) A velocity gradient of the CO gas along the minor axis (figures 9b and 11) is found. It seems unlikely that the red- and blue-shifted components indicate motion of the gas parallel to the galactic plane for the cylindrical structure vertically extending from the plane. The northwestern side of the plane is shown to be the near side, because the optical light at the southeastern side is more highly reddened and polarized due to the dust in the halo than at the northwestern side (Chesterman and Pallister 1980; Notni and Bronkalla 1983). Then the observed red- and blue-shifts seem to indicate an outflow of the gas nearly perpendicular to the disk.

These facts lead us to the idea that the molecular gas as well as the hot plasma are expanding out of the plane of the galaxy (figure 12). The expanding velocity depends on the inclination angle of the plane. Although the angle is not well determined, the values of 82° (Lynds and Sandage 1963), 71°–75° (Blackman et al. 1979), 70°–80°, most likely 78° (Notni and Bronkalla 1983), and 75°–82° (Unger et al. 1984) have been evaluated (90° is edge-on). We here consider i=70°–85° as the inclination angle of the plane, 80° being a most likely value. For this angle, the expansion velocity is 100–500 km s^{-1} (200 km s^{-1} for i=80°) from the observed line-of-sight velocity

Table 3. Parameters of the expanding molecular gas.

Mass (H_2)[a]	$5\times10^7\ M_\odot$
Velocity[b]	100–500 km s^{-1}
Height	$>\pm500$ pc
Energy[c]	$(1\text{–}13)\times10^{55}$ erg

[a] Within the region of $|z|>100$ pc and $|r|<500$ pc.
[b] Assuming the inclination angle of 70°–85° (90° is edge-on).
[c] The kinetic and gravitational energy.

(V_{rel}=30–40 km s^{-1}) relative to the center, simply assuming that the velocity vector is perpendicular to the galactic plane. This expansion velocity exceeds the escape velocity of the galaxy (100–150 km s^{-1}). The mass of the molecular gas in the halo of M82 at $|z|>100$ pc and $|r|<500$ pc is estimated to be about $5\times10^7\ M_\odot$. In this case, the kinetic energy E_{kin} and gravitational energy E_{gra} of the expanding molecular gas are $(0.5\text{–}13)\times10^{55}$ erg, most likely 2×10^{55} erg, and 0.5×10^{55} erg, respectively. If one third of the H I gas [$5\times10^7\ M_\odot$ (Crutcher et al. 1978)], the H II gas [$7\times10^7\ M_\odot$ (Willner et al. 1977)], and the X-ray emitting gas [$10^7\ M_\odot$ (Watson et al. 1984)] are flowing out from the galactic disk as the molecular gas, the total expansion energy becomes about twice the above value. The parameters of the expanding gas are summarized in table 3.

The most plausible origin of the gas outflow is an energy supply from supernova explosions in the galactic disk. The total kinetic energy E_{kin} (SN) released into the interstellar space during t_s by supernovae is given by

$$E_{kin}(SN)=\int_{-t_s}^{0}\gamma_{SN}(t)E_0(SN)p\,dt\ , \qquad (1)$$

where $\gamma_{SN}(t)$ is the supernova rate at t, E_0(SN) the initial total energy of a supernova event, and p the ratio of the kinetic energy released into the interstellar space to E_0(SN). We adopt 10^{51} erg for E_0(SN) and 0.03 for p (Chevalier 1974). The supernova rate γ_{SN} is assumed to be proportional to the rate of star formation (SFR). Rieke et al. (1980) proposed a star burst model of the M82 nucleus, where the rate of star formation has an exponential decay [SFR$\propto\exp(-t/\alpha)$] and the initial mass function has a power law. The time constant α is 2×10^7 yr and the duration t_s of the burst star formation is 5×10^7 yr as derived from a best-fitting model to explain the total luminosity, the absolute magnitude at 2.2 μm, and the Lyman continuum flux. Therefore, the supernova rate $\gamma_{SN}(t)$ is given by

$$\gamma_{SN}(t)=\gamma_{SN}(0)\exp(-t/\alpha)\quad(-t_s<t<0), \qquad (2)$$

where $\gamma_{SN}(0)$ is the present rate of supernova events, and α is 2×10^7 yr. The value of $\gamma_{SN}(0)$ is estimated to be 0.1 SN yr^{-1} from total nonthermal emission of M82 (Kronberg and Wilkinson 1975), 0.2 SN yr^{-1} from the far-infrared luminosity (Kronberg and Sramek 1985), 0.3 SN yr^{-1} from a star burst model (Rieke et al. 1980), and 0.35 SN yr^{-1} from the 8–13 μm emission (Jones and Rodriguez-Espinosa 1984). We here adopt 0.3 SN yr^{-1} for the present supernova rate $\gamma_{SN}(0)$. From equations (1) and (2), the total kinetic energy E_{kin}(SN) of 2×10^{57} erg may be released into the interstellar space

for $t_s=5\times10^7$ yr. The expanding gas with the velocity of 100–500 km s^{-1} requires the traveling time of $(1\text{–}7)\times10^6$ yr from the galactic disk up to the observed area of $|z|\simeq700$ pc (figures 2 and 4) For $t_s=(1\text{–}7)\times10^6$ yr, the kinetic energy E_{kin}(SN) becomes $(1\text{–}8)\times10^{55}$ erg, which is comparable to the expansion energy of the molecular gas [$E_{kin}+E_{gra}\simeq(1\text{–}13)\times10^{55}$ erg]. The kinetic energy supplied by SN explosions is sufficient to blow up the observed molecular gas into the halo of M82. Another fraction of the released SN energy may be used to heat the interstellar matter to high temperature, and the heated gas will expand into a halo, forming there Hα filaments and an X-ray halo. Watson et al. (1984) and Unger et al. (1984) have also suggested that the Hα and X-ray emitting gas is flowing out from the nuclear region and its energy originates in supernova explosions. Chevalier and Clegg (1985) have given an analytical solution for the wind with a velocity of ~2000 km s^{-1} deduced from radio spectra (Seaquist et al. 1985).

It has been pointed out that the optical light scattered by outward-moving particles should show redshift on both sides of the galactic plane, which contradicts the explosion hypothesis advocated by Lynds and Sandage (1963) and Burbidge et al. (1964). However, some authors (O'Connell and Mangano 1978; Axon and Taylor 1978) argued that the inner (<1 kpc) filaments do not shine by the scattered light but the emission is intrinsic, because the emission lines observed toward the inner filaments and the central region of the galaxy are different in the intensity ratios of Hα/[N II] and [S II]/[N II] and in the line widths. In this case, the observed blue- and red-shifts of the optical light are not against the expanding model, but strongly suggest the actual outflow of the ionized gas.

Although ejections of molecular gas off the galactic plane from the central region have been known only in M82 (CO; this paper) and NGC 253 (OH; Turner 1985), such a phenomenon might be commonly seen in galaxies undergoing rapid star formation. This means that any galaxies might have blown off gas from their disks at the initial stage of their formation when the rate of star formation was extremely high. Mass loss of galaxies in their early time would affect the evolutionary history of the galaxies, and suggests larger masses of primordial galaxies than the present masses. This also suggests the existence of the intergalactic gas clouds if they failed to recollapse to form stars. In the case of M82, the total kinetic energy of supernova explosions released into the interstellar space during the past 5×10^7 yr (duration time t_s of burst star formation) is about 2×10^{57} erg, which is at least one order of magnitude greater than the present expansion energy of $(1\text{–}13)\times10^{55}$ erg. Therefore, M82 ought to have blown off the gas with a mass greater than $10^9\,M_\odot$ for t_s (cf. the present expanding mass is $5\times10^7\,M_\odot$), or the mean mass-loss rate was as high as $10^9\,M_\odot/5\times10^7$ yr$\simeq20\,M_\odot$ yr^{-1}. This implies that a considerable fraction, one tenth of the total mass $\sim10^{10}\,M_\odot$ within 3 kpc of the center, has been lost in the last $\sim10^8$ yr. It is actually known that the molecular gas extends into the halo of M82 up to 2′–3′ (1′$\simeq$ 950 pc at the distance of 3.25 Mpc) from the galactic plane (Stark and Carlson 1984; Young and Scoville 1984). The mass of molecular hydrogen in the region of |the distance from the galactic plane|$>45''$ (i.e., outside of our mapped area) and the distance from the galactic center $<3'$ is estimated to be $1.3\times10^8\,M_\odot$ or $8.4\times10^8\,M_\odot$ from figure 5 of Young and Scoville (1984), where the former value is for small optical

depth (<1) by the same procedure as in subsection 3.2 and the latter for large optical depth with the I_{CO}/H_2 conversion factor of Young and Scoville (1982). The actual mass is probably between these two values. Furthermore there exists 10^9 $M_\odot$ of H I surrounding M82 (Gottesman and Weliachew 1977; Cottrell 1977). Although the H I gas has been considered to be the gas captured from the neighboring galaxy M81 during the encounter with it (cf. Cottrell 1977), H I holes along the Hα filaments (Cottrell 1977), which resemble a cavity of CO in the halo, suggest that the H I gas is also flowing out from M82. Therefore, the H_2 gas and a fair amount of the H I gas in the halo would have been due to mass loss from M82.

6. Summary

The observations of the CO ($J=1$–0) emission of M82 with the spatial resolution of 16″ resolved the distribution of the molecular gas in the galaxy and presented new aspects of the behavior of the molecular gas in the active sites of star formation around the nucleus. Main results and conclusions are summarized as follows:

1. The distribution of the CO intensity in the central region is resolved into two peaks. An axisymmetric model reveals a ring structure of the molecular gas around the distance of 200 pc from the nucleus. The molecular ring corresponds to the region of current star formation. Inside this ring the molecular gas is depleted and shows a "central hole."

2. The spurlike extension of the molecular gas is running almost perpendicular to the galactic plane toward the halo at least up to $\pm 30''$ (± 500 pc) above and below the plane. The spurs lie just outside the Hα filaments and the X-ray halo and appear to make a hollow cylinder. This cylinder has a velocity gradient along the minor axis of the galaxy. These facts fit a model in which the molecular gas in M82 is expanding out of the galactic plane with the velocity of 100–500 km s^{-1}. The expansion energy of $(1\text{–}13)\times 10^{55}$ erg can be supplied continuously by supernova explosions in the central region of M82.

3. The molecular gas in M82 is in the form of hot ($\simeq 40$ K), small ($\simeq 6$ pc), and low-mass ($\simeq 6\times 10^3$ $M_\odot$) clouds like hot cores in molecular clouds associated with the H II regions in our Galaxy. This is probably due to the extremely high rate of star formation.

If the molecular gas is expanding out of the galactic plane, dust grains would be also flowing out. Actually it is well known that many patchy dust lanes are distributed in the halo of the galaxy. Submillimeter or far-infrared observations with high resolution are useful to confirm the cavity wall perpendicular to the galactic plane. CO spurs extending toward the halo are almost perpendicular to the galactic disk. Hα filaments in the northern halo are elongated parallel to each other and perpendicularly to the disk up to a height of 4 kpc (e.g., Deharveng and Pellet 1970). M. Umemura and K. Shibata (private communication) stress the importance of magnetic fields to such well-collimated gases ejected from nuclei of star burst galaxies. Radio observations of polarization in the halo of M82 might make clear whether magnetic fields contribute to the collimation of the gases.

The authors thank Dr. V. Stanger and Dr. P. J. McCarthy for sending X-ray images and Hα photographs of M82, respectively. They appreciate valuable discussions with Dr. G. Rydbeck. They also thank the referee, Dr. K. Y. Lo whose comments have improved the contents of the paper.

References

Axon, D. J., and Taylor, K. 1978, *Nature*, **274**, 37.
Berkhuijsen, E. M. 1984, *Astron. Astrophys.*, **140**, 431.
Bingham, R. G., McMullan, D., Pallister, W. S., White, C., Axon, D. J., Scarrott, S. M. 1976, *Nature*, **259**, 463.
Blackman, C. P., Axon, D. J., and Taylor, K. 1979, *Monthly Notices Roy. Astron. Soc.*, **189**, 751.
Burbidge, E. M., Burbidge, G. R., and Rubin, V. C. 1964, *Astrophys. J.*, **140**, 942.
Burton, W. B., and Gordon, M. A. 1978, *Astron. Astrophys.*, **63**, 7.
Chesterman, J. F., and Pallister, W. S. 1980, *Monthly Notices Roy. Astron. Soc.*, **191**, 349.
Chevalier, R. A. 1974, *Astrophys. J.*, **188**, 501.
Chevalier, R. A., and Clegg, A. W. 1985, *Nature*, **317**, 44.
Combes, F., and Gerin, M. 1985, *Astron. Astrophys.*, **150**, 327.
Condon, J. J. 1983, *Astrophys. J. Suppl.*, **53**, 459.
Cottrell, G. A. 1977, *Monthly Notices Roy. Astron. Soc.*, **178**, 577.
Crutcher, R. M., Rogstad, D. H., and Chu, K. 1978, *Astrophys. J.*, **225**, 784.
Deharveng, J. M., and Pellet, A. 1970, *Astron. Astrophys.*, **9**, 181.
de Vaucouleurs, G., and Buta, R. 1980, *Astrophys. J. Suppl.*, **44**, 451.
de Vaucouleurs, G., and de Vaucouleurs, A. 1964, *Reference Catalogue of Bright Galaxies* (University of Texas Press, Austin).
Dickman, R. L. 1975, *Astrophys. J.*, **202**, 50.
Elvius, A. 1969, *Lowell Obs. Bull.*, **7**, 117.
Frerking, M. A., Langer, W. D., and Wilson, R. W. 1982, *Astrophys. J.*, **262**, 590.
Fukunaga, M. 1983, *Publ. Astron. Soc. Japan*, **35**, 173.
Fukunaga, M. 1984, *Publ. Astron. Soc. Japan*, **36**, 417.
Gérin, M., Combes, F., and Nakai, N. 1987, submitted to *Astron. Astrophys.*
Gottesman, S. T., and Weliachew, L. 1977, *Astrophys. J.*, **211**, 47.
Harper, D. A., and Low, F. J. 1973, *Astrophys. J. Letters*, **182**, L89.
Heckathorn, H. M. 1972, *Astrophys. J.*, **173**, 501.
Holmberg, E. 1950, *Medd. Lunds Astron. Obs. Ser. II*, No. 128.
Holmberg, E. 1958, *Medd. Lunds Astron. Obs. Ser. II*, No. 136.
Jaffe, D. T., Becklin, E. E., and Hildebrand, R. H. 1984, *Astrophys. J. Letters*, **285**, L31.
Jones, B., and Rodriguez-Espinosa, J. M. 1984, *Astrophys. J.*, **285**, 580.
Knapp, G. R., Phillips, T. G., Huggins, P. J., Leighton, R. B., and Wannier, P. G. 1980, *Astrophys. J.*, **240**, 60.
Kronberg, P. P., and Biermann, P. 1983, in *Supernova Remnants and Their X-Ray Emission, IAU Symp. No. 101*, ed. J. Danziger and P. Gorenstein (Reidel, Dordrecht), p. 583.
Kronberg, P. P., Biermann, P., and Schwab, F. R. 1981, *Astrophys. J.*, **246**, 751.
Kronberg, P. P., Biermann, P., and Schwab, F. R. 1985, *Astrophys. J.*, **291**, 693.
Kronberg, P. P., and Sramek, R. A. 1985, *Science*, **227**, 28.
Kronberg, P. P., and Wilkinson, P. N. 1975, *Astrophys. J.*, **200**, 430.
Leung, C. M., and Liszt, H. S. 1976, *Astrophys. J.*, **208**, 732.
Liszt, H. S. 1982, *Astrophys. J.*, **262**, 198.
Lo, K. Y., Cheung, K. W., Masson, C. R., Phillips, T. G., Scott, S. L., and Woody, D. P. 1987, *Astrophys. J.*, **312**, 574.
Lo, K.Y., Phillips, T.G., Knapp, G.R., Wootten, H.A., and Huggins, P. 1980, *Bull. American Astron. Soc.*, **12**, 859.

Lynds, C. R., and Sandage, A. R. 1963, *Astrophys. J.*, **137**, 1005.
McCarthy, P. J., Heckman, T., and van Breugel, W. 1987, *Astron. J.*, **93**, 264.
Nakai, N., Hayashi, M., Handa, T., Sofue, Y., Hasegawa, T., and Sasaki, M. 1986, *Publ. Astron. Soc. Japan*, **38**, 603.
Nilson, P. 1973, *Uppsala Astron. Obs. Ann.*, **6**.
Nordsieck, K. H. 1973, *Astrophys. J.*, **184**, 719.
Notni, P., and Bronkalla, W. 1983, in *Internal Kinematics and Dynamics of Galaxies, IAU Symp. No. 100*, ed. E. Athanassoula (Reidel, Dordrecht), p. 67.
O'Connell, R. W., and Mangano, J. J. 1978, *Astrophys. J.*, **221**, 62.
Olofsson, H., and Rydbeck, G. 1984, *Astron. Astrophys.*, **136**, 17.
Oort, J. H. 1977, *Ann. Rev. Astron. Astrophys.*, **15**, 295.
Phillips, T. G., and Huggins, P. J. 1977, *Astrophys. J.*, **211**, 798.
Rickard, L. J., and Harvey, P. M. 1984, *Astron. J.*, **89**, 1520.
Rickard, L. J., Palmer, P., Morris, M., Turner, B. E., and Zuckerman, B. 1977, *Astrophys. J.*, **213**, 673.
Rieke, G. H., Lebofsky, M. J., Thompson, R. I., Low, F. J., and Tokunaga, A. T. 1980, *Astrophys. J.*, **238**, 24.
Rubin, V. C., and Ford, W. K., Jr. 1970, *Astrophys. J.*, **159**, 379.
Sandage, A. 1961, *The Hubble Atlas of Galaxies* (Carnegie Institution of Washington, Washington, D.C.), plate 41.
Sanders, R. H. 1979, in *The Large-Scale Characteristics of the Galaxy, IAU Symp. No. 84*, ed. W. B. Burton (Reidel, Dordrecht), p. 383.
Sanders, D. B., Solomon, P. M., and Scoville, N. Z. 1984, *Astrophys. J.*, **276**, 182.
Schwarz, M. P. 1984, *Monthly Notices Roy. Astron. Soc.*, **209**, 93.
Scoville, N. Z., Becklin, E. E., Young, J. S., and Capps, R. W. 1983, *Astrophys. J.*, **271**, 512.
Seaquist, E. R., Bell, M. B., and Bignell, R. C. 1985, *Astrophys. J.*, **294**, 546.
Solinger, A. B. 1967, *Astron. J.*, **72**, 830.
Solinger, A.B., and Markert, T. 1975, *Astrophys. J.*, **197**, 309.
Solinger, A., Morrison, P., and Markert, T. 1977, *Astrophys. J.*, **211**, 707.
Solomon, P. M., and Sanders, D. B. 1980, in *Giant Molecular Clouds in the Galaxy*, ed. P. M. Solomon and M. G. Edmunds (Pergamon Press, Oxford), p. 41.
Stark, A. A., and Carlson, E. R. 1984, *Astrophys. J.*, **279**, 122.
Stark, A. A., and Wolff, R. S. 1979, *Astrophys. J.*, **229**, 118.
Sutton, E. C., Masson, C. R., Phillips, T. G. 1983, *Astrophys. J. Letters*, **275**, L49.
Tammann, G. A., and Sandage, A. 1968, *Astrophys. J.*, **151**, 825.
Telesco, C. M., and Harper, D. A. 1980, *Astrophys. J.*, **235**, 392.
Turner, B. E. 1985, *Astrophys. J.*, **299**, 312.
Ulich, B. L., and Haas, R. W. 1976, *Astrophys. J. Suppl.*, **30**, 247.
Unger, S. W., Pedlar, A., Axon, D. J., Wilkinson, P. N., and Appleton, P. N. 1984, *Monthly Notices Roy. Astron. Soc.*, **211**, 783.
Visvanathan, N. 1974, *Astrophys. J.*, **192**, 319.
Visvanathan, N., and Sandage, A. 1972, *Astrophys. J.*, **176**, 57.
Watanabe, M., Kodaira, K., and Okamura, S. 1982, *Astrophys. J. Suppl.*, **50**, 1.
Watson, M. G., Stanger, V., and Griffiths, R. E. 1984, *Astrophys. J.*, **286**, 144.
Weliachew, L., Fomalont, E. B., and Greisen, E. W. 1984, *Astron. Astrophys.*, **137**, 335.
Wilkinson, P. N., and de Bruyn, A. G. 1984, *Monthly Notices Roy. Astron. Soc.*, **211**, 593.
Willner, S. P., Soifer, B. T., and Russell, R. W. 1977, *Astrophys. J. Letters*, **217**, L121.
Young, J. S., and Scoville, N. Z. 1982, *Astrophys. J.*, **258**, 467.
Young, J. S., and Scoville, N. Z. 1984, *Astrophys. J.*, **287**, 153.